

An improvement in mass flux convective parameterizations and its impact on seasonal simulations using a coupled model

Ahmed Elsayed Yousef¹ · M. Azhar Ehsan¹ · Mansour Almazroui¹ · Mazen E. Assiri¹ · Abdulrahman K. Al-Khalaf¹

Received: 19 April 2015 / Accepted: 26 October 2015 / Published online: 9 November 2015
© Springer-Verlag Wien 2015

Abstract A new closure and a modified detrainment for the simplified Arakawa–Schubert (SAS) cumulus parameterization scheme are proposed. In the modified convective scheme which is named as King Abdulaziz University (KAU) scheme, the closure depends on both the buoyancy force and the environment mean relative humidity. A lateral entrainment rate varying with environment relative humidity is proposed and tends to suppress convection in a dry atmosphere. The detrainment rate also varies with environment relative humidity. The KAU scheme has been tested in a single column model (SCM) and implemented in a coupled global climate model (CGCM). Increased coupling between environment and clouds in the KAU scheme results in improved sensitivity of the depth and strength of convection to environmental humidity compared to the original SAS scheme. The new scheme improves precipitation simulation with better representations of moisture and temperature especially during suppressed convection periods. The KAU scheme implemented in the Seoul National University (SNU) CGCM shows improved precipitation over the tropics. The simulated precipitation pattern over the Arabian Peninsula and Northeast African region is also improved.

1 Introduction

The simulated climate (Wu et al. 2008; Kim and Kang 2008) is strongly dependent on the representation of deep convection

and its detailed implementation (Kang and Hong 2008) in global climate models (GCMs). A convective parameterization generally consists of the following three components: (1) cloud model: to explicate the effect of convection on the environment, (2) closure: to determine the intensity of convection, and (3) triggering: to determine when to activate the convection scheme (Emanuel et al. 1994). Most convective schemes in current GCMs use the mass flux formulation because of its physical basis and internally consistent treatment of cloud-associated physical processes.

The closure in convection parameterization is a fundamental but still a controversial problem as reviewed in Yano et al. (2013b). Various approaches have been presented to improve the convection closure, and simulated precipitation is quite sensitive to their details (Negggers et al. 2004; Bechtold et al. 2014; Yang et al. 2014). Convective available potential energy (CAPE) is commonly considered as an important variable controlling convection (Nordeng 1995; Bechtold et al. 2001) and is used in many current deep convection schemes (Arakawa and Schubert 1974; Moorthi and Suarez 1992; Zhang and Mcfarlane 1995; Zhang 2002). However, observations (e.g., Barkidija and Fuchs 2013) and cloud-resolving models (e.g., Yang et al. 2014) show that rainfall and cloud base mass flux has almost no correlation with CAPE. On the other hand, precipitation rate is well correlated with moisture in observations (Barkidija and Fuchs 2013). Moisture-based closure (Kuo 1974) has been criticized because of its causality problem (Emanuel et al. 1994). Derbyshire et al. (2004) compared the relationship between environmental humidity and convection in single-column models with convection schemes to that in cloud-resolving models. They concluded that the sensitivity of most schemes to environmental humidity is too low compared to cloud-resolving models. Convection schemes that are more sensitive to environmental relative humidity have been proposed and show improvements in global precipitation

✉ M. Azhar Ehsan
mehsan@kau.edu.sa

¹ Center of Excellence for Climate Change Research/Department of Meteorology, King Abdulaziz University, P.O. Box 80208, Jeddah 21589, Saudi Arabia

patterns (e.g., Zhang and Mu 2005; Bechtold et al. 2008; Chikira and Sugiyama 2010; Kim and Kang 2011).

The aim of the current study is to improve the simplified relaxed Arakawa–Schubert (SAS) mass flux convection scheme (Numaguti et al. 1995) by including the effect of environmental relative humidity. The modified closure depends on the buoyancy force and is controlled by the relative humidity of the surrounding environment. The cloud base mass flux represents the convection intensity and is driven by both cloud and environment properties. The cloud base mass flux is generated and intensifies according to the integral of buoyancy force (CAPE) between cloud base and cloud top and is controlled by mean environment relative humidity (Bechtold et al. 2008; Chikira and Sugiyama 2010). The simple representation of cloud fraction in the cloud base mass flux and use of moisture threshold improves the simulation of the different convection stages. Higher tops and stronger mass flux magnitudes occur when the column is more humid. During dry conditions, an updraft parcel easily loses its buoyancy by entraining dry environment air, inhibiting deep convection, consistent with observations and cloud-resolving models (Derbyshire et al. 2004; Kuang and Bretherton 2006). In addition, modifying the detrainment at cloud tops by its environment relative humidity eradicates the problem of excessive moistening of upper atmospheric layers.

The paper is structured as follows. Section 2 describes the formulation of the modified SAS scheme. Section 3 discusses the models, experiment design, and observational datasets. In Sect. 4.1, the modified scheme is tested in an idealized single-column model and compared with the original SAS scheme and observation. In Sect. 4.2, the modified scheme is implemented in a coupled GCM for the seasonal prediction of the 5-month season of November–December–January–February–March (NDJFM) for the years 1996, 1997, and 1998. Summary and conclusions are given in Sect. 5.

2 Description of the modifications

The primary equations relating the interaction between cumuli and the large-scale environment variables follow the original Arakawa–Schubert scheme and the simplifications described in Numaguti et al. (1995). An ensemble of cumulus cloud types are assumed to have same cloud base but distinct cloud tops characterized by different entrainment rates. Each cloud entrains mass from the environment up to the cloud top, where the entire mass detrains. Each cloud is completely described by the mass flux at its base and the entrainment rate. The following two modifications are proposed to the simplified Arakawa–Schubert scheme.

First, to improve the mass flux intensity, a new closure is proposed that integrates the equation for the vertical motion of each cloud subensemble from cloud base to cloud top,

assuming the updraft vertical velocity at the cloud top is zero. According to Simpson and Wiggert (1969) and Gregory (2001), the updraft vertical velocity equation is:

$$\frac{1}{2} \frac{\partial}{\partial Z} W_u^2 = \alpha B - \beta \varepsilon W_u^2, \quad (1)$$

where α and β are dimensionless constants and Z is height. W_u and B are the updraft velocity and the buoyancy of the cloud air parcel, respectively. The buoyancy “ B ” of the cloud parcel is defined by:

$$B = \frac{g(\theta_{vu} - \theta_v)}{\theta_v} - g(l_c + P_c), \quad (2)$$

where θ_{vu} and θ_v are the virtual potential temperatures inside the cloud and its grid mean environmental value, respectively, and g is the gravitational constant. The term $(l_c + P_c)$ is expressed as the summation of the mass of cloud water and rain water (this represents the drag of hydrometeors). Gregory (2001) suggested a fractional entrainment rate “ ε ” based on budgets of cumulus vertical velocity

$$\varepsilon = \frac{C_\varepsilon \alpha g}{W_u^2} B, \quad (3)$$

where C_ε is a dimensionless constant parameter ranging from 0 to 1 and is the conversion factor for the kinetic energy generated by buoyancy to entrained air. Using a simple dependency of C_ε on environmental humidity from Kim and Kang (2011), we can define C_ε , as follows:

$$C_\varepsilon = \left(\frac{1}{RH_T} - 1 \right) \times \frac{q_s^T}{q_s^B},$$

where q_s^T is the environmental saturated specific humidity at the cloud top, q_s^B is the saturation-specific humidity at the cloud base level, and RH_T is the environmental relative humidity at the cloud top level for every subensemble. During cloudy conditions, the entrainment rate decreases as the cloud top level increases, increasing the depth of the cloud. In a drier environment, the entrainment rate increases near the cloud base level, which suppresses convection and decreases the depth of the cloud.

Integrating Eq. (1) from cloud base to cloud top using Eq. (3), and assuming that at the cloud top, W_{ut} is 0, gives:

$$W_{ub}^2 = \int_{z_b}^{z_t} (1 - C_\varepsilon g \beta) 2 \alpha B dz, \quad (4)$$

where W_{ub} is the updraft velocity of the cloud base. Using the relation between updraft vertical velocity and cumulus mass flux $M = \rho a_c W_{ub}$, (4) becomes:

$$M_{cb} = \rho a_c \left[\alpha \int_{z_b}^{z_t} (1 - C_\varepsilon g \beta) 2 B dz \right]^{1/2}, \quad (5)$$

where ρ is the air density and a_c is the cloud fraction defined as:

$$a_c = 1 - \frac{RH_m - RH_1}{1 - RH_1}, \quad (6)$$

where RH_m is the mean environment relative humidity, and RH_1 is a critical relative humidity, known as cloud threshold. Cloud thresholds have been widely used in convective parameterization schemes to suppress convection (Moorthi and Suarez 1992; Zhang and Mu 2005) in drier environments. Following many sensitivity tests, the default RH_1 value used in this study is 70 %. If $RH_1 < 70\%$, the cloud fraction is assumed to be 0.

The new cloud base mass flux (convection intensity) is driven by both cloud and environment properties as follows:

1. CAPE is positive to trigger convection and intensifies by the generated CAPE between cloud base and cloud top.
2. Cloud base mass flux is a function of a_c which represents the cloud environment moistening using threshold value 70 % for mean environment relative humidity between cloud base of the deepest subensemble and its top. Convection is suppressed when the boundary layer is too dry. On the other hand, the convective cloud deepens when sufficient moisture is available.
3. Cloud base mass flux decays by entrainment, a function of buoyancy force at different levels in the atmosphere. In addition, the entrainment rate increases as environment relative humidity decreases to suppress deep convection.

Second, the detrainment at cloud top has also been modified by its environment relative humidity to overcome the problem of excessive moistening of the upper atmospheric layers. A number of studies show the sensitivity of detrainment to the relative humidity and stability of the free troposphere (e.g., Derbyshire et al. 2011; Böing et al. 2012; De Rooy et al. 2013). For instance, Böing et al. (2012) examined the mechanisms that determine detrainment in deep cumulus convection in a set of 90 high-resolution large-eddy simulations. They found that detrainment impacts cloud top height and precipitation rates, and depends strongly on the relative humidity and stability of the free troposphere. Here, the detrainment factor (D) in the modified SAS scheme also depends on the moistening parameter C_ε , which also appears in the expression for the entrainment. The modified detrainment D' is

$$D' = C_\varepsilon D$$

The modified detrainment decreases when $\frac{q_T}{q_S}$ decreases and as cloud top level increases to overcome the problem of moistening the upper levels associated with SAS scheme. D' increases in drier environment, which increases the moistening in the upper layers.

3 The model and experiment design

3.1 The model

The Seoul National University coupled global climate model (SNU CGCM) is used here to perform the seasonal simulations described in Sect. 4.2 The SNU CGCM consists of the SNU AGCM coupled with the Geophysical Fluid Dynamics Laboratory (GFDL) ocean model MOM2.2. The SNU CGCM includes the simplified version of relaxed Arakawa–Schubert scheme for deep convection (Numaguti et al. 1995), a large-scale condensation scheme with a prognostic microphysics parameterization of total cloud liquid water (Le Treut and Li 1991) and the non-precipitating shallow convection scheme of Tiedtke (1984). The CGCM also involves the land surface model by Bonan (1996), a non-local PBL/vertical diffusion scheme by Holtslag and Boville (1993) and atmospheric radiation parameterized as in Nakajima et al. (1995). The ocean model, MOM2.2 has 32 vertical levels with 23 levels in the upper 450 m. A mixed layer model (Noh and Kim 1999) is embedded within the ocean model. Further details can be found in Lee et al. (2003) and Kug et al. (2007).

A single column version of the SNU AGCM is used to test the new King Abdulaziz University (KAU) convection scheme. The single-column model (SCM) framework is an important tool for investigating and developing parameterization schemes (Randall et al. 1996). Although the SCM is insufficient for understanding all of the impacts of a convection scheme on model simulation, it does characterize the performance of the scheme in different convective situations.

3.2 Experiment design

Before introducing a new parameterization into the full model and assessing its impact on either forecasting performance or climate modeling, it is desirable to understand its working in the SCM framework. Here, the SCM is used in two experiments. In the first experiment, the standard SAS cumulus convection scheme (CTL) is used, and in the second experiment, the SCM uses the new KAU scheme (MOD).

We compare the two convection schemes (CTL and MOD) in the SCM framework using data from the Tropical Ocean and Atmosphere Coupled Ocean Atmosphere Response Experiment (TOGA COARE, Webster and Lukas 1992). The TOGA COARE is a special observation program for tropical convection, and the data represents an average over the TOGA COARE intensive flux array, a region of about 400 by 250 km with lat/lon ranges of 2° S–4° S and 155° E–158° E. The initial conditions and forcing data are obtained from the TOGA COARE and the Global Energy and Water Cycle Experiment (GEWEX) Cloud System Study (GCSS). The aim of the GCSS project is to support the development of improved parameterization schemes related to cloud processes

for large-scale models (Randall et al. 2000). The SCM experimentation setup described here is similar to the one in Kim and Kang (2011).

4 Performance of modified (KAU) scheme

Before a detailed comparison of the CTL and MOD (KAU) schemes, we summarize the problem of the standard convection scheme in the SNU GCM as discussed in Kim and Kang (2011). Kim and Kang (2011) compared time-averaged, vertical profiles of relative humidity from the 40-year European Center for Medium Range Weather Forecast (ECMWF) re-analysis and from a 10-year (1999–2008) atmospheric model intercomparison project (AMIP) type simulation of the SNU AGCM, over deep tropics and also over the TOGA COARE region. Area-averaged relative humidity over both regions showed similar biases (dryness from mid to lower troposphere). They attributed this bias to the model convection scheme (SAS), in particular to its poor sensitivity to environmental relative humidity. The present study differs from Kim and Kang (2011), considering multiple cloud types as in the original Arakawa–Schubert scheme (Arakawa and Schubert 1974), while Kim and Kang (2011) used bulk mass flux (Tiedtke 1989).

4.1 Single-column model results

4.1.1 Comparison of relative humidity and related thermodynamics quantities

The sensitivity of the MOD (KAU) convection scheme to moisture is compared to that of the CTL by focusing on profiles of relative humidity and temperature from two different periods in the TOGA COARE data. Figure 1a, b shows the humidity profile simulated by the CTL and MOD (KAU) convection schemes during periods A and B. Period A (29 November–10 December 1992) shows slowly increasing precipitation, and period B (9 January–21 January 1993) shows active, suppressed, and transition states of convection. First, we discuss the vertical profile of relative humidity without the detrainment modification (purple curve: No Dtrn). Even without the detrainment modification, there are improvements in the vertical profile of humidity in lower and upper levels, but the upper layers are too moist, and the lower troposphere is too dry (Fig. 1). To overcome this problem, we assume a simple dependency of detrainment on environmental humidity (Böing et al. 2012). Sensitivity runs with different values of RH_T were used to find the value that gives the best simulation of the environmental heating and moistening. The modified detrainment produces relative humidity profiles that are closer to the observations than “No Dtrn” or “CTL”. The

improvement in humidity profile is more pronounced during period A (Fig. 1a) than during period B (Fig. 1b).

To investigate the effect of the modified detrainment on temperature, the heating associated with different RH_T values and “No Dtrn” are calculated and shown in Fig. 2a, b. The CTL temperature profile shows less bias than the MOD (KAU) profile in the lower troposphere during period A (Fig. 2a) but a greater bias in the middle and upper troposphere. The MOD (KAU) and “No Dtrn” temperature profiles are quite close to each other during period A, except when $RH_T = 80\%$ (Fig. 2a). During period B, bias in the CTL temperature profile increases, while the MOD (KAU) temperature profile shows more or less similar bias in its different sensitivity simulations (Fig. 2b). Vertical profiles of temperature indicate that MOD reduces the temperature bias over all atmosphere levels during the two periods. The simulations of temperature and humidity profiles with smallest bias (OBS-MOD) have an RH_T value of 55% as shown in Figs. 1 and 2.

To highlight the improvement, the difference of horizontal time series of relative humidity simulated by the MOD (KAU) scheme (for $RH_T = 55\%$) and CTL scheme during two periods is shown in Fig. 3. The vertical profiles of relative humidity simulated by the CTL and MOD schemes are also shown. Figure 3b, e shows the relative humidity bias (dry lower troposphere and wet upper troposphere) simulated by the CTL scheme during periods A and B, respectively. For instance, considering the mostly dry phase 1st December to 3rd 1992 during period A, the CTL scheme dries out the dry layers, so the lower troposphere remains dry for the remainder of period A (Fig. 3b). In contrast, the MOD (KAU) scheme gradually moistens the lower troposphere after this dry phase (Fig. 3a). The difference in the response for the similar environmental conditions is due to the lack of moisture sensitivity in the CTL scheme, which simulates deep convection and completely dries out the lower troposphere in dry conditions. This bias is reduced in MOD by including the sensitivity of convection to environmental moisture conditions through strengthening the interaction between environment and cloud (Fig. 3c). The difference between MOD and CTL in period B is presented in Fig. 3d, e. Although the difference between the two schemes is not large, the bias of the MOD scheme is relatively less than that of the CTL scheme (Fig. 3f). Nevertheless, the results from period A which contains very dry phases are convincing and show quite good improvement in simulating the relative humidity.

We now focus on the updraft mass flux simulations of the CTL and MOD (KAU) schemes. Figure 4 shows the updraft mass flux, a proxy of convective activity, simulated by the CTL and MOD during both periods. During period A, the MOD mass flux weakens and gradually increases with the moistening of the troposphere from 1 December 1992 (Fig. 4a). However, the mass flux simulated by CTL shows quite high values even during the dry period, and quite strong

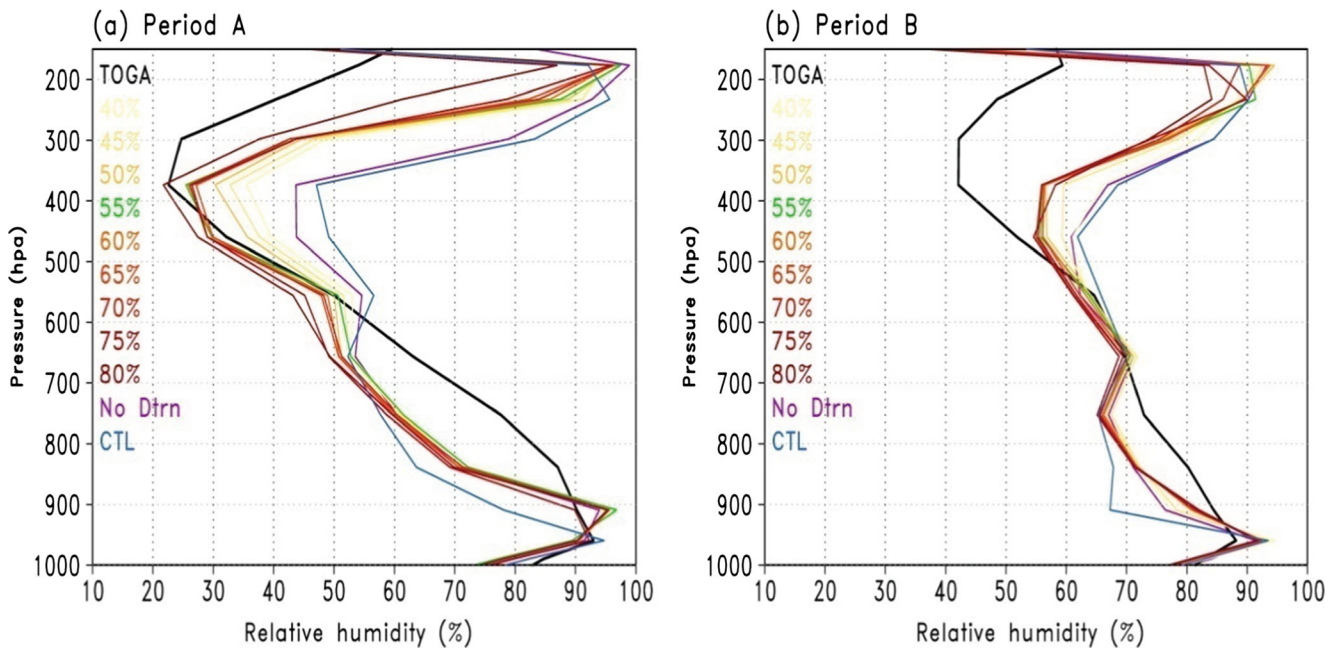


Fig. 1 The vertical profile of relative humidity as simulated by the CTL/SAS and MOD/KAU schemes for the subperiods A (a) and B (b) of TOGA COARE IFA data. Different colors show different relative humidity threshold values used to control detrainment. Unit of relative humidity is (%)

mass flux is observed during the moistening period (Fig. 4b). During period B, the mass flux simulated by MOD scheme weakens during the suppressed period and intensifies with the intensification of the convection cloud activity for the period 15 to 20 Jan. with maximum on 19 Jan. Thus, the MOD scheme simulates well the moderate and deep updraft mass fluxes in wet columns and the weak updraft mass fluxes in dry conditions (Fig. 4c). The cloud mass flux in the CTL scheme has a number of maximum values for different days, even

during the period of suppressed convection (Fig. 4d). This behavior occurs because the CTL scheme assumes that all kinds of cumulus clouds are characterized by buoyancy force (Arakawa and Schubert 1974) and are relatively unaffected by environmental conditions. Adequate sensitivity of convection to environmental conditions is important for the development of different convection stages in a convective scheme.

The difference between the cloud mass fluxes generated by CTL and MOD arise basically from the differing cloud

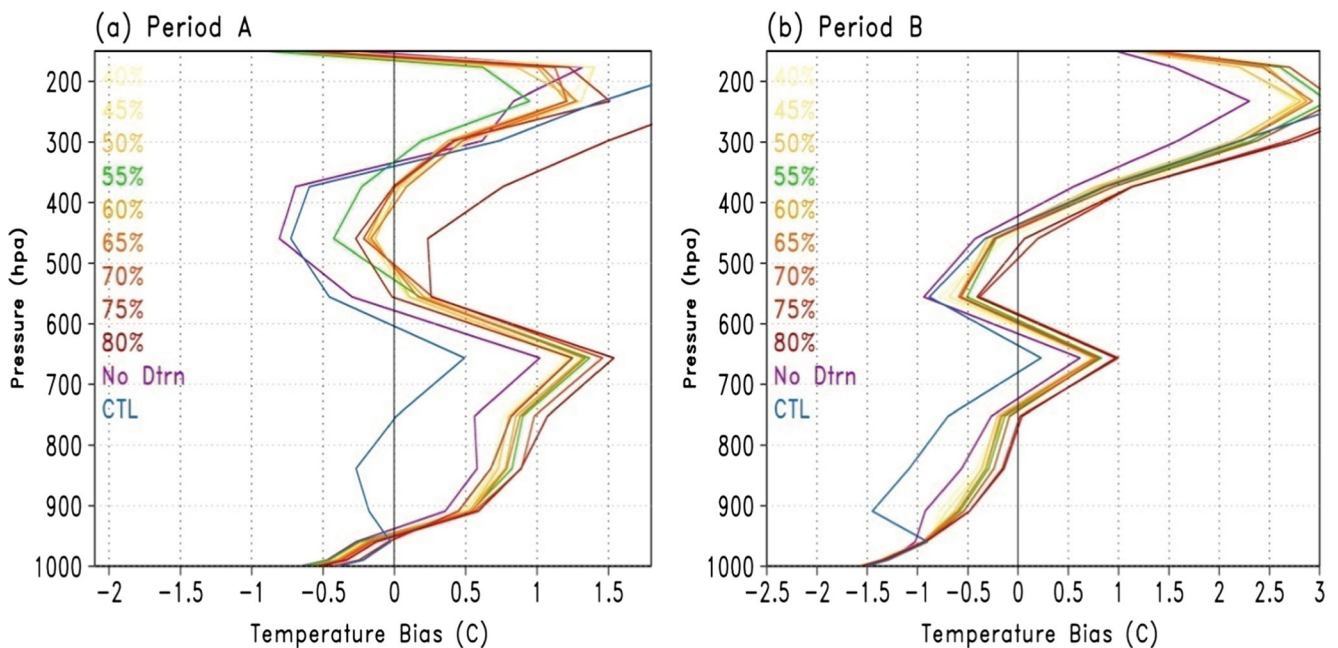


Fig. 2 The vertical profile of temperature bias simulated by the CTL/SAS and MOD/KAU schemes for the sub periods A (a) and B (b) of TOGA COARE IFA data. Different colors show different relative humidity threshold values used to control detrainment. Unit of temperature bias is (°C)

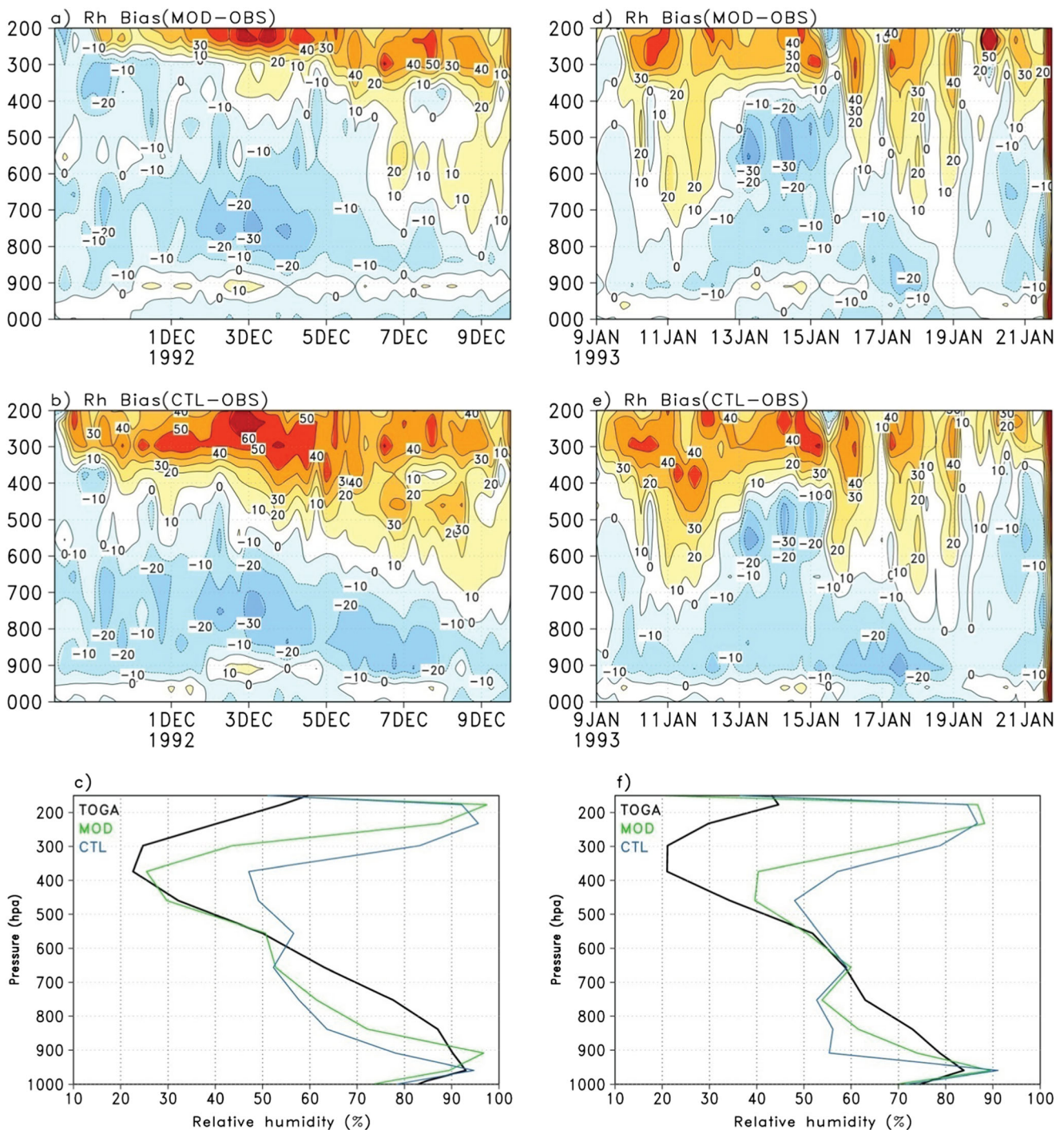


Fig. 3 The difference of horizontal time series of relative humidity as simulated by the MOD (for $RH_T = 55\%$) and CTL schemes, from the observation. The vertical profiles of relative humidity as simulated by the

SAS and MOD schemes are also shown. Period A (left column) and period B (right column). Unit of relative humidity is (%)

base mass flux definitions. Comparing the cloud base mass flux distribution of both schemes with the observed distribution of rainfall shows that the MOD scheme cloud base mass flux is (not shown) moderately correlated (0.6) with the observed precipitation distribution, while the correlation of the CTL cloud mass base flux is poor (0.3).

The gradual increase of cloud top and strengthening of mass flux is better simulated in the MOD scheme than in the CTL scheme because the MOD cloud base mass flux depends on both CAPE and mean column relative humidity which define cloud fraction, while the CTL scheme depends only on CAPE.

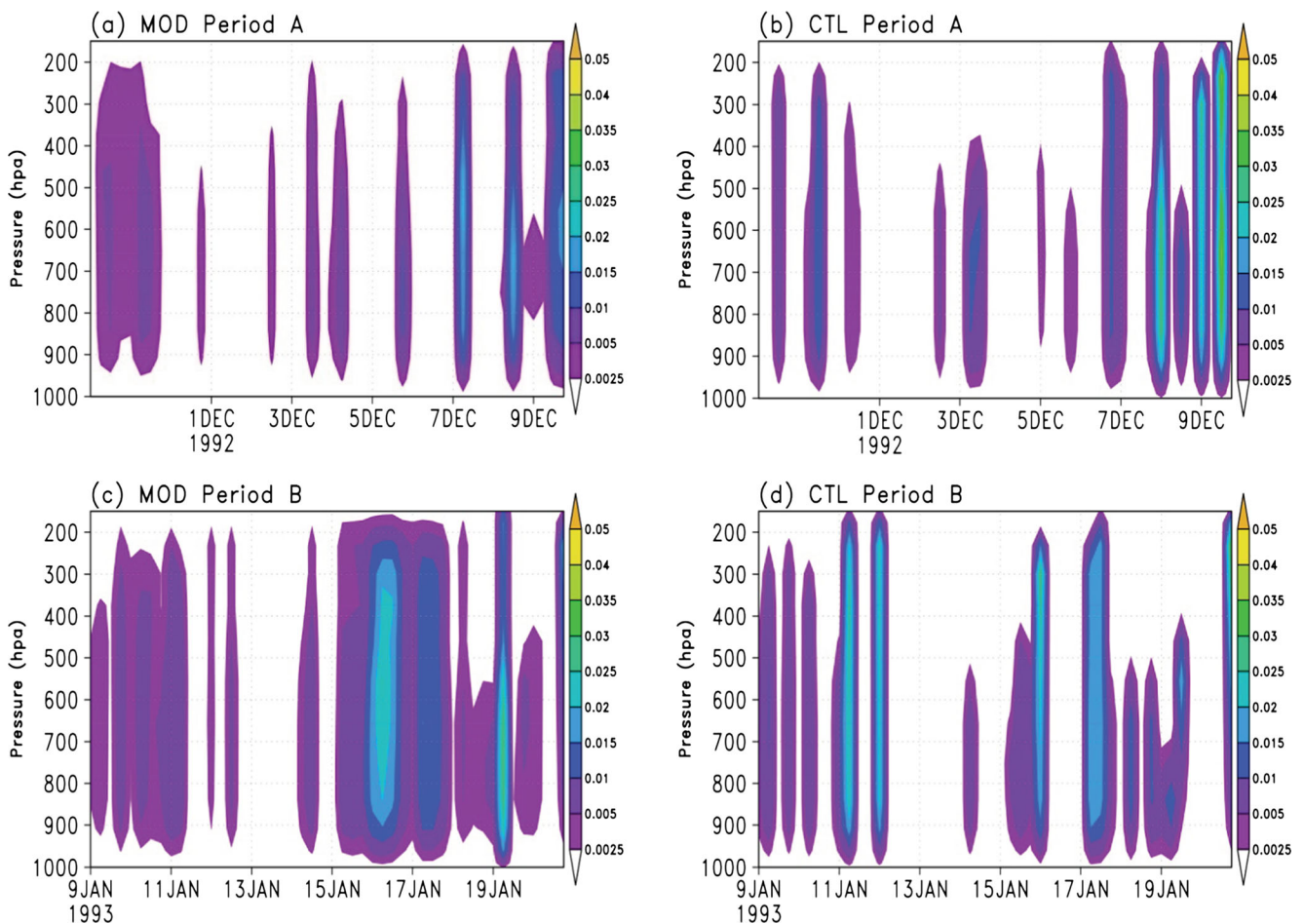


Fig. 4 Time series for the updraft mass flux simulated by the CTL/SAS and MOD/KAU schemes **a, b** for period A and **c, d** for period B. Unit of mass flux is $\text{kg m}^{-2} \text{s}^{-1}$

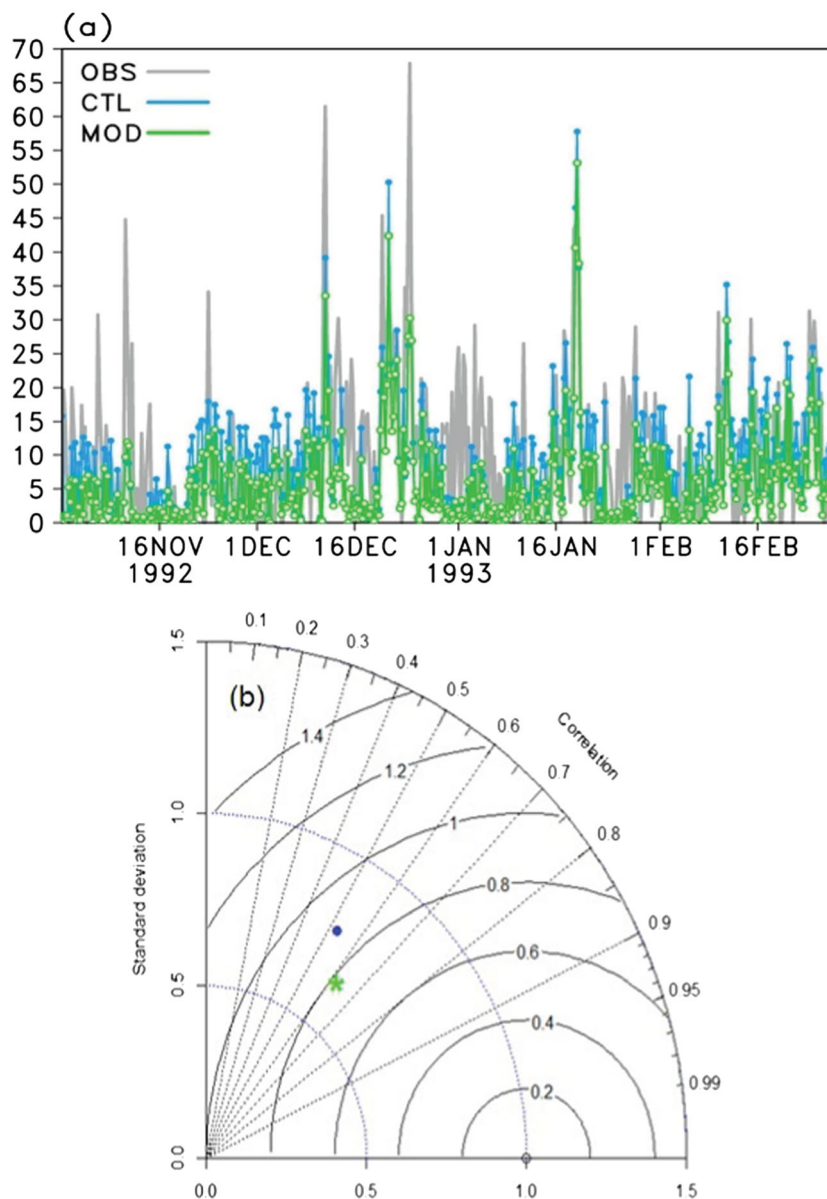
4.1.2 Improvement in precipitation

We now compare the CTL and MOD precipitation simulations. Figure 5a shows the precipitation time series simulated by the CTL and MOD convection schemes in the SCM framework along with observations for the entire TOGA COARE period. The SCM with the CTL and MOD schemes simulates total precipitation relatively well. A Taylor diagram (Taylor 2001) is employed to compare the ability of CTL and MOD schemes during the whole period (Fig. 5b). A Taylor diagram shows how closely the simulated precipitation matches observation as measured by the correlation coefficient (CC; azimuthal angle), the ratio of standard deviations (radial distance), and root mean square (RMS) error (distance between the observation and simulation points). Here, the 6-h precipitation simulated by CTL and MOD schemes is represented by a blue filled circle and a green asterisk, respectively. The standard deviation of the simulated precipitation is low compared to the observation, suggesting that the spatial variance simulated by the two schemes is smaller than observed. Overall, the rainfall simulation of the MOD scheme is better than that

of the CTL scheme during the TOGA COARE period, having higher CC and lower RMS error. The differences between the two schemes are further illustrated using the two periods (A and B) with differing states of convection.

Figure 6a, b shows a comparison of the observed and simulated precipitation from the CTL and MOD schemes during periods A and B, respectively. The two schemes, CTL (blue) and MOD (green), are quite good in simulating precipitation during the two periods (Fig. 6). For instance, during period A, both schemes simulate precipitation relatively well, and the CC of the CTL and MOD schemes with observations is 0.50 and 0.47, respectively. During period B, the CTL scheme simulates precipitation during the active phase well but does not perform well in the other phases. In particular, the CTL scheme produces too much precipitation during the periods of Jan. 12–14 and Jan. 21–22 of period B. In contrast, the MOD scheme captures the precipitation distribution well in terms of both magnitude and pattern during all of period B. The peaks during the transitional and active convection are reproduced but slightly underestimated. The correlations of the MOD and CTL schemes with the observations during period B are 0.89 and 0.68, respectively.

Fig. 5 **a** The time series of observation (*gray*), SAS/CTL (*blue*) and MOD/KAU (*green*) and **b** the Taylor diagram for the precipitation, *dot* (*blue*) and *asterisk* (*green*) represents the SAS and the KAU schemes. Time series for the precipitation is obtained from the whole 4 months TOGA COARE data (Nov. 1992 to Feb. 1993)



The comparatively good association of the MOD scheme-simulated precipitation with observation could be due to the induction of the moisture sensitivity. By formulating the entrainment and detrainment in terms of cloud and environment variables in an appropriate manner, the MOD scheme allows interaction between the cloud and environment in a more effective and appropriate way, resulting in improved simulated precipitation.

4.2 Coupled global climate model seasonal prediction results

The performance of the MOD/KAU convection scheme has been examined for seasonal prediction using the SNU CGCM. The initial conditions for the seasonal prediction experiments are constructed by the nudging method, which drives the model

solution toward the observations. Temperature and salinity obtained from the Global Ocean Data Assimilation System (GODAS; Behringer and Xue 2004) reanalysis are nudged from the surface to a depth of 500 m with a 5-day relaxation time scale. The atmospheric data was obtained from the NCEP reanalysis-II (Kanamitsu et al. 2002a). The model has a resolution of T106 L45 (triangular truncation at wave number T106 in the horizontal and 45 terrain-following sigma layers in the vertical). Six-month seasonal predictions starting in October of 1996, 1997, and 1998 are performed to compare the two convection schemes. We discard the first forecast month and analyze the 5-month season Nov.–March (NDJFM).

The zonal mean values of simulated NDJFM precipitation for the three years 1996/1997, 1997/1998, and 1998/1999 are shown in Fig. 7a–c. Figure 7a–c indicates that the mean GPCP

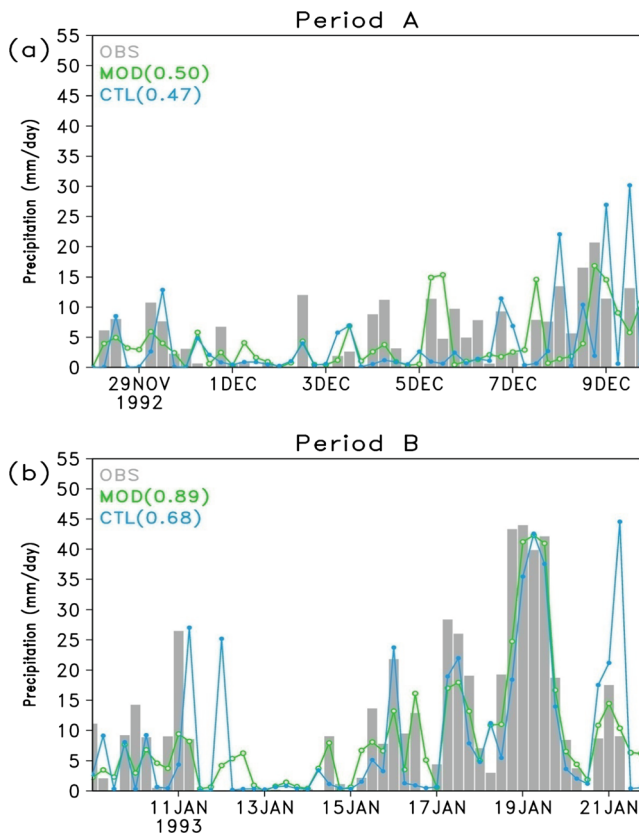


Fig. 6 Time series for the precipitation obtained from the TOGA COARE data (bars), and simulated by CTL/SAS (blue) and MOD/KAU (green) convection schemes **a** for the first sub-period A and **b** the same as (a) but for the second subperiod B. Unit of precipitation is mm/day

rainfall (black curves) from November to March 1996/1997 and 1998/1999 have two maxima over the tropical domains, with enhancement of rain over the southern part relative to the northern part, except during 1997/1998 where a single peak is noted (Picaut et al. 2002). Figure 7 reveals that the simulations from the MOD/KAU (green) and CTL/SAS (blue) schemes capture the two peaks quite well over the tropical area, as well as the two over the middle latitudes. The KAU scheme simulates the zonal features better than the CTL scheme during 1996/1997 (Fig. 7a), by capturing the two peaks over the tropical domain with higher amounts in the southern part. The CTL scheme shows similar peaks north and south of the equator. In Fig. 7b, the KAU scheme has one peak over the equator and similar zonal distribution to that of GPCP with higher rainfall values, but CTL still has the two peaks over the tropical domain. Figure 7c shows approximately the same zonal distribution of KAU and CTL for the year 1998/1999. Thus, an improvement is noticed in the predicted distribution of precipitation using the KAU scheme (slightly overestimated values).

Figure 8 highlights the effect of the KAU scheme on the horizontal distribution of mean rainfall. The simulations with CTL scheme (Fig. 8c, d) have a number of known deficiencies such as the South Pacific Convergence Zone (SPCZ) is weak over

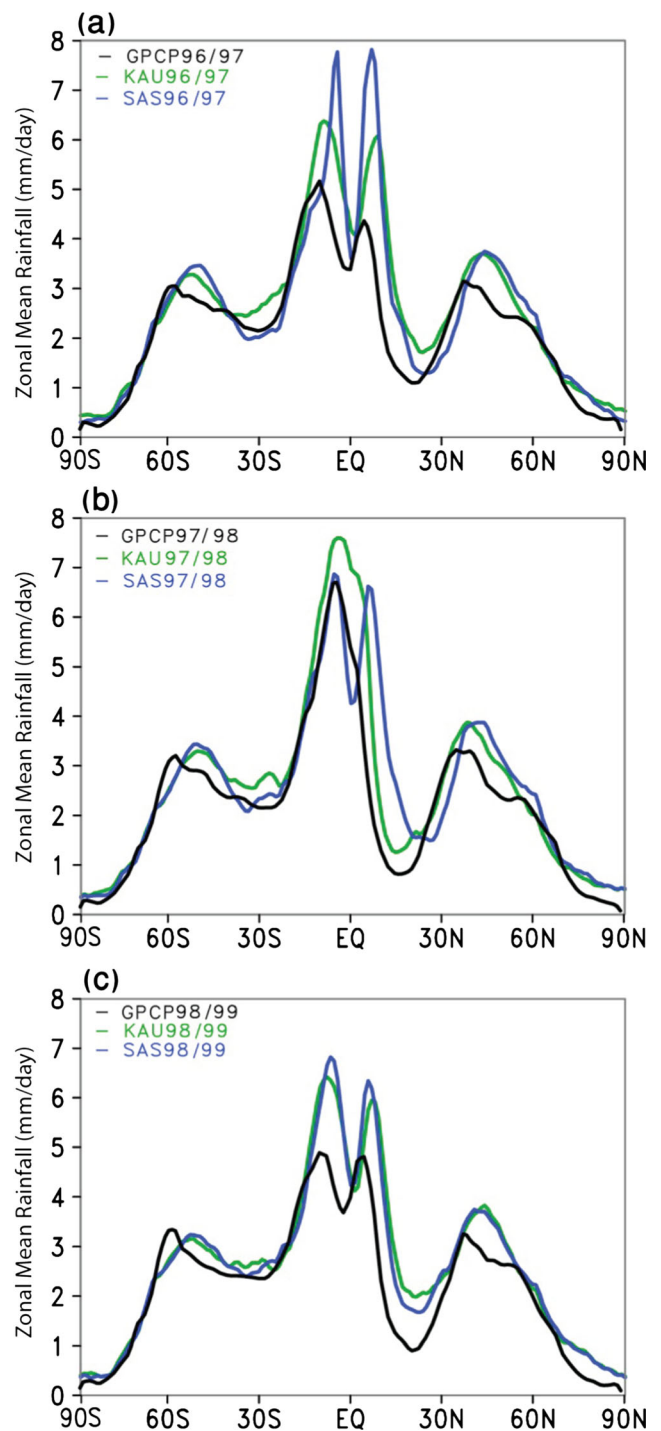


Fig. 7 Zonal cross-section of precipitation averaged for the months November–March for the years **a** 1996/1997 GPCP (black), SAS (blue), and KAU (green), **b** the same as (a) but for 1997/1998, **c** the same as (a) but for 1998/1999. Unit of precipitation is mm/day

the western and central Pacific, shifted more northward, and it appears as a double ITCZ in the western region and Indian Ocean. The simulations with KAU scheme (Fig. 8e, f) are able to capture the prominent band-like structure in the observations, such as the ITCZ and the SPCZ. For both years, the simulated precipitation is too large over the western and central parts of the Pacific Ocean

and too small over the eastern Indian Ocean; it is particularly high over the western Indian Ocean. Thus, the main differences between the predicted precipitation from CTL and KAU schemes are the strengthening of the SPCZ in the central tropical Pacific and the enhancement of the ITCZ precipitation band in the western Indian Ocean (shifted slightly southward), with higher magnitudes than the GPCP.

Over Saudi Arabia, heavy precipitation was observed during 1997/1998 and dry conditions during 1998/1999. These 2 years provide contrasting assessment of the two convection schemes (SAS and KAU) in a coupled GCM seasonal prediction framework. Observations show high precipitation over the northern part of the Arabian Gulf and extending over the central and northeastern areas of Saudi Arabia in 1997/1998. During 1998/1999, overall drying appears except in the northern part of the Arabian Gulf. The KAU convection scheme

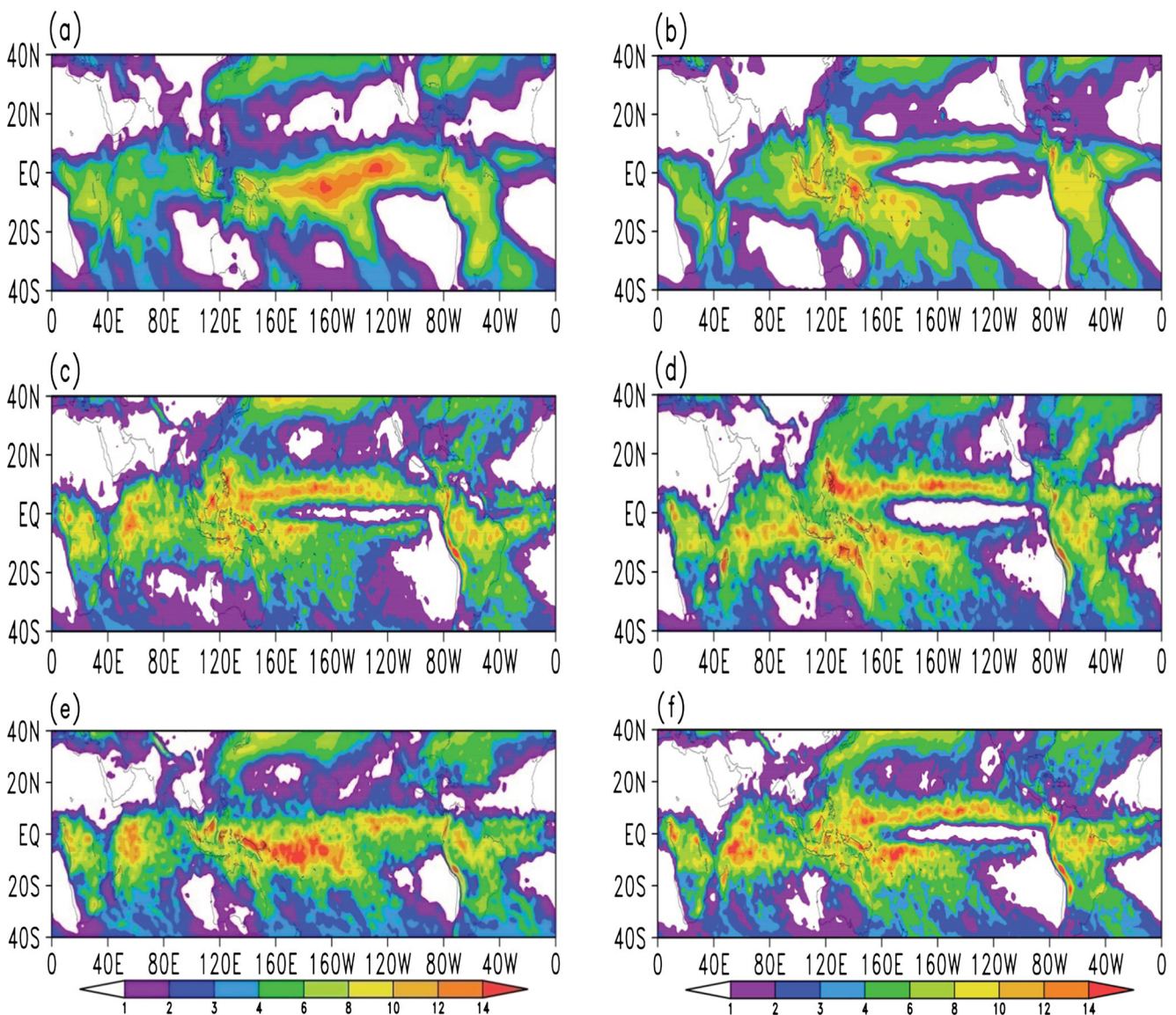


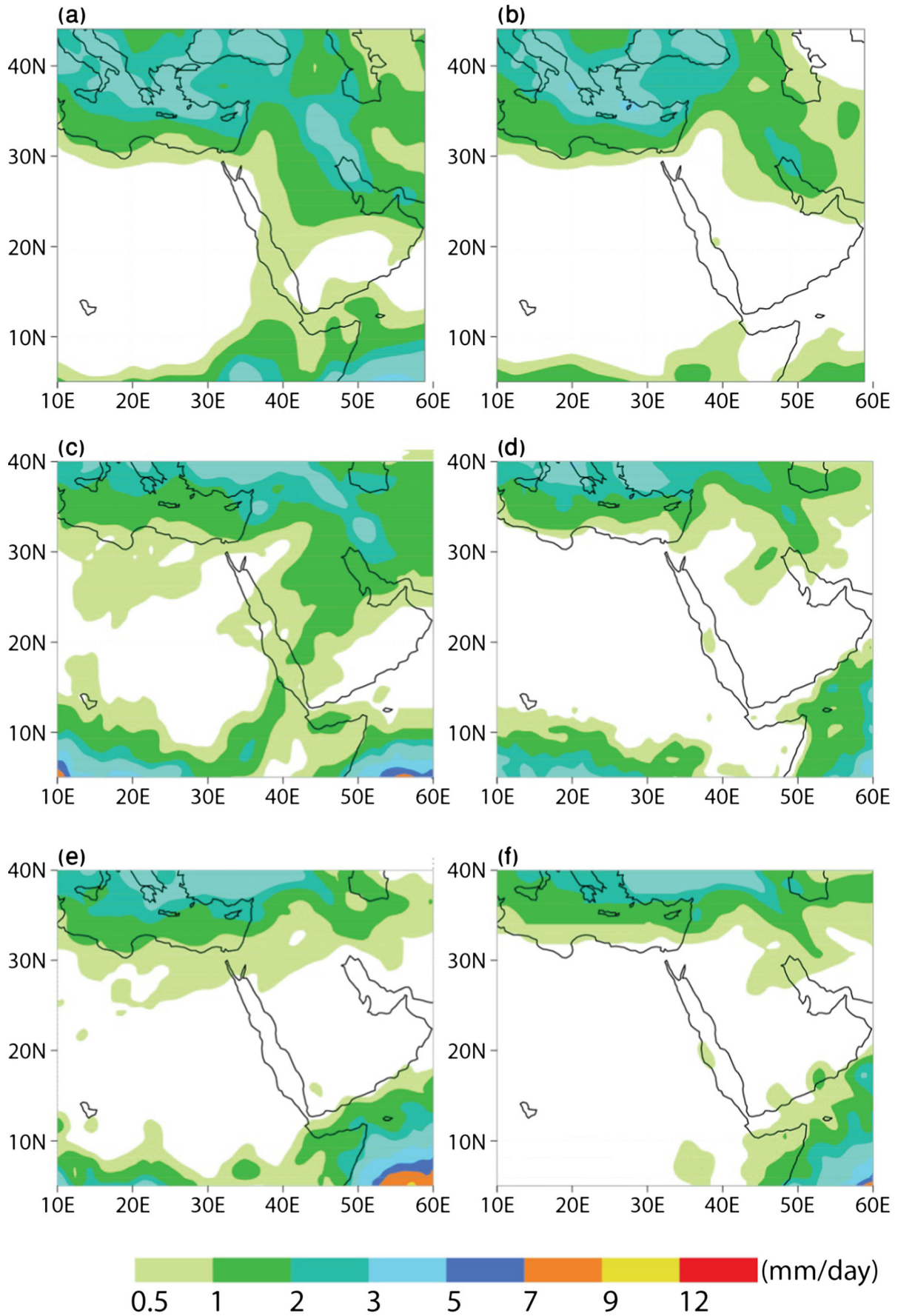
Fig. 8 Horizontal distribution of precipitation over the globe, averaged for the months of November–March of the years 1997/1998 and 1998/1999, for **a, b** observation, **c, d** the SAS scheme, and **(e, f)** the KAU scheme. Unit of precipitation is mm/day

Fig. 9 Horizontal distribution of precipitation over the Arabian Peninsula averaged for the months of November–March of the years 1997/1998 and 1998/1999, for **a, b** observation, **c, d** the KAU scheme, and **(e, f)** the SAS scheme

(Fig. 9c, d) predicted well the spatial distribution and magnitude of precipitation over the Arabian Peninsula and Northeast Africa. The CTL scheme poorly predicted both distribution and magnitude of the precipitation over the region (Fig. 9e, f).

5 Summary and conclusions

The aim of this study is to improve the simulation of deep convection within climate models. Our main objective is to assess the ability of the KAU scheme to handle suppressed



and active convection clouds. We have implemented two main parameters to control the cloud base mass flux: the availability of buoyancy force and the sufficient moisture in the cloud column; and then depicted their effects on the convective development. In addition, the detrainment at cloud tops is modified by its environmental relative humidity to remove the problem of moistening of the upper atmosphere layers.

The modified convection scheme is evaluated in the SCM framework by specifying the observed horizontal and vertical advection of temperature and specific humidity as a forcing from TOGA COARE data. We select two periods (A and B) from TOGA which include suppressed and active convection regimes and the transition between them. SCM results with CTL (SAS) and MOD (KAU) convection schemes are compared with observed variables. SAS shows a dry (wet) bias in the lower (upper) troposphere. The KAU scheme provides a better simulation of the updraft mass flux and relative humidity compared to the SAS scheme. Single-column model precipitation is also improved with the KAU scheme. The impact of modifications on seasonal predictions was examined for the winter months (November to March) of 1996, 1997, and 1998. The prediction results obtained with KAU scheme shows improvement in the distribution of precipitation amounts over the tropical oceans and over the Arabian Peninsula.

Our results suggest that a conventional convection scheme is still able to simulate the observed relationship between convection and environmental moisture by improving the convection scheme itself. One of the most important factors in achieving this is the detrainment parameterization (currently a poorly understood process), which heavily impacts cloud top height and precipitation rates (Böing et al. 2012). Impacts of the KAU scheme on long-term climate simulations of different seasons will be examined in future work.

Acknowledgments The authors would like to acknowledge the Center of Excellence for Climate Change Research (CECCR), Department of Meteorology, Deanship of Graduate Studies and Deanship of Scientific Research, King Abdulaziz University (KAU), Jeddah, Saudi Arabia, for providing the necessary support to carry out this study. We thank anonymous reviewer for making insightful comments that lead to substantial improvements in the final version of the paper. Computation for the work described in this paper was supported by King Abdulaziz University's High Performance Computing Center (Aziz Supercomputer: <http://hpc.kau.edu.sa>).

References

- Arakawa A, Schubert WH (1974) Interaction of a cumulus ensemble with the large-scale environment, part I. *J Atmos Sci* 31:674–704
- Barkidija S, Fuchs Z (2013) Precipitation correlation between convective available potential energy, convective inhibition and saturation fraction in middle latitudes. *Atmos Res* 124:170–180
- Behringer DW, Xue Y (2004) Evaluation of the global ocean data assimilation system at NCEP: the Pacific Ocean In: Eighth symposium on integrated observing and assimilation systems for atmosphere, ocean, land surface. AMS 84th annual meeting, Seattle, Washington, 11–15 Jan
- Bechtold P, Bazile E, Guichard F, Mascart P, Richard E (2001) A mass flux convection scheme for regional and global models. *Q J R Meteorol Soc* 127:869–886
- Bechtold P, Kohler M, Jung T, Doblas-Reyes F, Leutbecher M, Rodwell MJ, Vitart F, Balsamo G (2008) Advances in simulating atmospheric variability with the ECMWF model: from synoptic to decadal time-scales. *Q J R Meteorol Soc* 134:1337–1351
- Bechtold P et al. (2014) Representing equilibrium and non equilibrium convection in large-scale models. *J Atmos Sci* 71:734–753
- Böing SJ, Siebesma AP, Korpershoek JD, Jonker HJJ (2012) Detrainment in deep convection. *Geophys Res Lett* 39:L20816. doi:10.1029/2012GL053735
- Bonan GB (1996) The land surface climatology of the NCAR land surface model coupled to the NCAR community climate model. *J Clim* 11:1307–1326
- Chikira M, Sugiyama M (2010) A cumulus parameterization with state-dependent entrainment rate. Part I: Description and Sensitivity to Temperature and Humidity Profiles *J Atmos Sci* 67:2171–2193
- Derbyshire SH, Beau I, Bechtold P, Grandpeix JY, Piriou JM, Redelsperger JL, Soares PMM (2004) Sensitivity of moist convection to environmental humidity. *Q J R Meteorol Soc* 130:3055–3079
- Derbyshire SH, Maidens AV, Milton SF, Stratton RA, Willett MR (2011) Adaptive detrainment in a convective parameterization. *Q J R Meteorol Soc* 137:1856–1871
- De Rooy WC, Bechtold P, Fröhlich K, Hohenegger C, Jonker H, Mironov D, Siebesma AP, Teixeira J, Yano JI (2013) Entrainment and detrainment in cumulus convection: an overview. *Q J R Meteorol Soc* 139:1–19
- Emanuel KA, Neelin JD, Bretherton CS (1994) On large-scale circulations in convecting atmospheres. *Q J R Meteorol Soc* 120:1111–1143
- Gregory D (2001) Estimation of entrainment rate in simple models of convective clouds. *Q J R Meteorol Soc* 127:53–72
- Holtzlag AAM, Boville BA (1993) Local versus non-local boundary layer diffusion in a global climate model. *J Clim* 6:1825–1842
- Kang HS, Hong SY (2008) Sensitivity of the simulated east Asian summer monsoon climatology to four convective parameterization schemes. *J Geophys Res* 113:D15119. doi:10.1029/2007JD009692
- Kanamitsu M, Ebisuzaki W, Woollen J, Yang SK, Hnilo JJ, Fiorino M, Potter GL (2002a) NCEP–DOE AMIP-II reanalysis (R-2) dynamical seasonal forecast system 2000. *Bull Amer Meteor Soc* 83:1631–1643
- Kim HM, Kang IS (2008) The impact of ocean–atmosphere coupling on the predictability of boreal summer intraseasonal oscillation. *Clim Dyn* 31:859–870
- Kim D, Kang IS (2011) A bulk mass flux convection scheme for a climate model: description and moisture sensitivity. *Clim Dyn* 38:411–429
- Kuang Z, Bretherton CS (2006) A mass-flux scheme view of a high resolution simulation of a transition from shallow to deep cumulus convection. *J Atmos Sci* 63:1895–1909
- Kug JS, Kang IS, Choi DH (2007) Seasonal climate predictability with tier-one and tier-two prediction systems. *Clim Dyn* 31:403–416
- Kuo YH (1974) Further studies of the parameterization of the influence of cumulus convection of large-scale flow. *J Atmos Sci* 31:1232–1240
- Le Treut H, Li ZX (1991) Sensitivity of an atmospheric general circulation model to prescribed SST changes: feedback effects associated with the simulation of cloud optical properties. *Clim Dyn* 5:175–187
- Lee MI, Kang IS, Mapes BE (2003) Impacts of cumulus convection parameterization on aqua-planet AGCM simulations of tropical intraseasonal variability. *J Meteorol Soc Jpn* 81:963–992
- Moorthi S, Suarez MJ (1992) Relaxed Arakawa-Schubert. A parameterization of moist convection for general circulation models. *Mon Weather Rev* 120:978–1002

- Neggers R, Siebesma A, Lenderink G, Holtslag A (2004) An evaluation of mass flux closures for diurnal cycles of shallow cumulus. *Mon Weather Rev* 132:2525–2538
- Nakajima T, Tsukamoto M, Tsushima Y, Numaguti A (1995) Modelling of the radiative process in an AGCM. In: Matsuno T (ed) *Climate system dynamics and modelling*, vol. 1–3. Univ. of Tokyo, Tokyo, pp. 104–123
- Nordeng TE (1995) Extended versions of the convective parameterization scheme at ECMWF and their impact on the mean and transient activity of the model in the tropics. *European Centre for Medium-Range Weather Forecasts*
- Noh Y, Kim HJ (1999) Simulations of temperature and turbulence structure of the oceanic boundary layer with the improved near surface process. *J Geophys Res* 104:15621–15634
- Numaguti A, Takahashi M, Nakajima T, Sumi A (1995) Development of an atmospheric general circulation model. In: Matsuno T (ed) *Climate system dynamics and modelling*, vol. 1–3. Univ. of Tokyo, Tokyo, pp. 1–27
- Picaut J, Hackert E, Busalacchi AJ, Murtugudde R, Lagerloef GSE (2002) Mechanisms of the 1997–1998 El Niño–La Niña, as inferred from space-based observations. *J Geophys Res* 107(C5). doi:10.1029/2001JC000850
- Randall DA, Xu KM, Somerville RJC, Iacobellis S (1996) Single column models and cloud ensemble models as links between observations and climate models. *J Clim* 9:1683–1697
- Randall DA, Curry J, Dwyer P, Krueger S, Miller M, Moncrieff M, Ryan B, Starr D, Rossow W, Tselioudis G, Wielicki B (2000) The second GEWEX cloud system study science and implementation plan. *IGPO Publ Ser* 34:45
- Simpson J, Wiggert V (1969) Models of precipitating cumulus towers. *Mon Weather Rev* 97:471–489
- Taylor KE (2001) Summarizing multiple aspects of model performance in a single diagram. *J Geophys Res* 106:7183–7192
- Tiedtke M (1984) The sensitivity of the time-mean large-scale flow to cumulus convection in the ECMWF model. 297–316.
- Tiedtke M (1989) A comprehensive mass flux scheme for cumulus parameterization in large-scale models. *Mon Weather Rev* 117:1779–1800
- Webster PJ, Lukas R (1992) TOGA COARE: the coupled ocean atmosphere response experiment. *Bull Am Meteorol Soc* 73:1377–1416
- Wu CM, Stevens B, Arakawa A (2008) What controls the transition from shallow to deep convection? *J Atmos Sci* 66:1793–1806
- Yang YM, Kang IS, Almazroui M (2014) A mass flux closure function in a GCM based on the Richardson number. *Clim Dyn* 42:1129–1138
- Yano JJ, Bister M, Fuchs Z, Gerard L, Phillips V, Barkidija S, Piriou JM (2013b) Phenomenology of convection-parameterization closure. *Atmos Phys Chem* 13:4111–4131
- Zhang GJ (2002) Convective quasi-equilibrium in midlatitude continental environment and its effect on convective parameterization. *J Geophys Res* 107. doi:10.1029/2001JD001005
- Zhang GJ, McFarlane NA (1995) Sensitivity of climate simulations to the parameterization of cumulus convection in the Canadian climate centre general circulation model. *Atmosphere-Ocean* 33:407–446
- Zhang GJ, Mu M (2005) Effects of modifications to the Zhang-McFarlane convection parameterization on the simulation of the tropical precipitation in the national center for atmospheric research community climate model, version 3. *J Geophys Res* 110:1–12